Chem
Europ

European C
Societies P

Check for
updates

Superacid Chemistry

Diprotonated Parabanic Acid: A Vicinal or 1,3-Dication?

Stefanie Beck,[a] Milica Raljic,[a] Christoph Jessen,[a] and Andreas J. Kornath*[a]

Abstract: Reacting parabanic acid with the superacidic systems XF/MF_5 (X = H, D; M = As, Sb) in different ratios, led to the formation of the mono- and diprotonated species. Salts in terms of $[C_3H_3N_2O_3][AsF_6]$, $[C_3H_3N_2O_3][SbF_6]$, $[C_3H_4N_2O_3][AsF_6]_2$, $[C_3H_4N_2O_3][SbF_6]_2$, $[C_3D_3N_2O_3][AsF_6]$ and $[C_3D_4N_2O_3][AsF_6]_2$ were obtained and characterized by low-temperature infrared and Raman spectroscopy. Single-crystal X-ray structure analyses were performed for $[C_3H_3N_2O_3][SbF_6]$ and $[C_3H_4N_2O_3][AsF_6]_2 \cdot$ 4HF. Additionally, quantum chemical calculations were carried out on the B3LYP/aug-cc-pVTZ level of theory for the mono- and dication. Mapped Electrostatic Potentials together with Natural Population Analysis charges were calculated in order to localize the two positive charges of the diprotonated parabanic acid. The diprotonated parabanic acid can be described as an 1,2-C,C-dication, stabilized by electron delocalization over the five-membered ring.

Introduction

Imidazolidine-2,4,5-trione, better known as parabanic acid, was prepared for the first time by *Woehler* and *Liebig* in 1838.[1] An established synthesis route is the reaction of urea with diethyl oxalate [Equation (1)].[2,3]
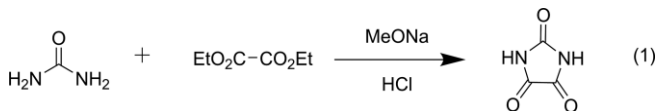
In a biological context, parabanic acid can be considered as the oxidation product of uric acid, which is the end-product of the nucleotide metabolism.[4,5] Parabanic acid is a heterocyclic compound with an imidazolidine skeletal structure, where the CH_2 groups are replaced by carbonyl groups. Thus, the molecule bears five potential basic centers. In this context, *Arca* et al. reported theoretical investigations on the electron delocalization and charge distribution.[6] Their results led to the assumption that protonations were possible on the carbonyl groups, as well as on the amine groups.

To the best of our knowledge, no isolated protonated species of parabanic acid has been reported in literature. In the course of our investigations on multiple protonations, we focus on two questions. First, to what extent it would be possible to protonate parabanic acid, and second, where the positive charges, in case of a higher protonated species, are located.

Results and Discussion

Synthesis of $[C_3H_3N_2O_3][MF_6]$ and $[C_3H_4N_2O_3][MF_6]_2$ (M = As, Sb)

The salts of the mono- and diprotonated parabanic acid were prepared according to Equations (2) and (3):
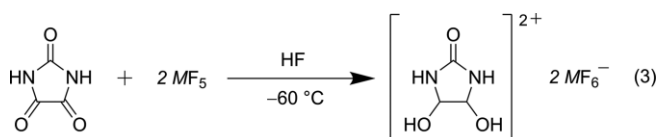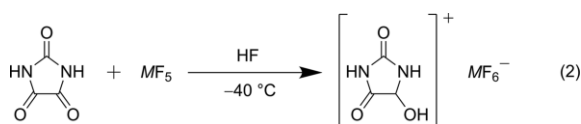
Firstly, the superacidic systems HF/AsF_5 and HF/SbF_5 were prepared using an excess of anhydrous hydrogen fluoride (aHF). Both mixtures were warmed up to –40 °C and homogenized to achieve complete solvation of the respective Lewis acid. After cooling down to –196 °C, parabanic acid was added to the frozen superacidic system under nitrogen atmosphere. The reaction mixture was warmed up to –40 °C (–60 °C, respectively), resulting in the formation of the protonated species. Excess aHF was removed at –78 °C under dynamic vacuum overnight. The salts were obtained as colorless solids, stable at room temperature under inert gas atmosphere.

The monoprotonated salts of parabanic acid $[C_3H_3N_2O_3]$-$[AsF_6]$ (**1**) and $[C_3H_3N_2O_3][SbF_6]$ (**2**) were obtained by using an equimolar amount of the starting material with respect to the Lewis acid.

Using a two-to-one ratio of Lewis acid, in terms of parabanic acid, the diprotonated species $[C_3H_4N_2O_3][AsF_6]_2$ (**3**) and

[a] S. Beck, M. Raljic, C. Jessen, Prof. Dr. A. J. Kornath
Department of Chemistry, Ludwig-Maximilian University München
Butenandtstr. 5–13, 81377 München, Germany
E-mail: andreas.kornath@cup.uni-muenchen.de
http://www.org.chemie.uni-muenchen.de/ac/kornath/
Supporting information and ORCID(s) from the author(s) for this article are
available on the WWW under https://doi.org/10.1002/ejoc.202000656.

EurJOC
European Journal of Organic Chemistry

Full Paper
doi.org/10.1002/ejoc.202000656

Chemistry Europe
European Chemical
Societies Publishing

$[C_3H_4N_2O_3][SbF_6]_2$ (**4**) were obtained. The salts (**3**) and (**4**) are stable up to –20 °C.

For vibrational spectroscopic studies, the deuterium isotopomers of both cations were prepared. The superacidic system DF/AsF_5 led to the formation of the corresponding deuterated species $[C_3D_3N_2O_3][AsF_6]$ (**5**) and $[C_3D_4N_2O_3][AsF_6]_2$ (**6**), respectively. The hydrogen atoms of the amine groups were entirely replaced by deuterium, as deuterium fluoride was used in large excess (100:1). The degree of deuteration approximates 98 %.

Even with an eight-to-one ratio of the stronger Lewis acid SbF_5, only the diprotonated species was obtained and, in this work, no triprotonated species was observed.

Crystal Structure of $[C_3H_4N_2O_3][AsF_6]_2$·4 HF (3)

The diprotonated species of parabanic acid $[C_3H_4N_2O_3][AsF_6]_2$·4HF (**3**) crystallizes in the monoclinic space group $C2/c$ with four formula units per unit cell. Figure 1 depicts the formula unit, with selected bond lengths and angles being summarized in Table 1.
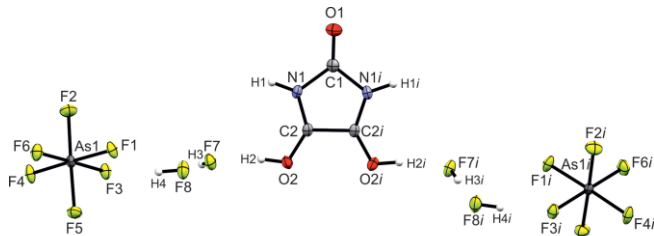
Figure 1. Formula unit of $[C_3H_4N_2O_3][AsF_6]_2$·4HF (50 % probability displacement ellipsoids). Symmetry code: $i = 1 - x$, y, $1.5 - z$.

Table 1. Selected bond lengths [Å] and angles [°] of $[C_3H_4N_2O_3][AsF_6]_2$·4HF (**3**) with estimated standard deviations in parentheses.[a]

Bond lengths [Å]			
O1–C1	1.167(3)	C2–C2i	1.511(3)
C1–N1	1.434(2)	C2–O2	1.253(2)
N1–C2	1.305(2)		
Bond angles [°]			
N1–C1–N1i	104.9(2)	O1–C1–N1	127.6(10)
C1–N1–C2	110.6(15)	O2–C2–N1	132.8(15)
N1–C2–C2i	106.9(9)	O2–C2–C2i	120.2(10)
Interatomic contacts D–A [Å]			
N1–(H1)···F4ii	2.765(2)	F7–(H3)···F8	2.449(2)
O2–(H2)···F7	2.479(2)	F8–(H4)···F3	2.511(1)

[a] Symmetry codes: $i = 1 - x, 1.5 - z$; $ii = 0.5 + x, 0.5 + y, 1 + z$.

Due to the twofold protonation, the C_{2v} symmetry of parabanic acid is conserved in the resulting dication. Both protonations are located on the respective neighboring carbonyl groups, O2/O2i. The protons were found in the difference Fourier synthesis and refined isotropically. However, the localization of the protons is not very meaningful. In consequence of the significant elongation of the C2–O2 (C2i–O2i respectively) bond length [1.253(2) Å], compared to the starting material,[7] the O-protonations are clearly confirmed. In contrast, the N1–C2 bond length becomes significantly shorter [1.305(2) Å]. The

third remaining carbonyl bond is significantly shortened, compared to the neutral compound,[7] and is, with a value of 1.167(3) Å, shorter than a formal CO double bond (1.19 Å).[8] Moreover, the C2–C2i bond length [1.511(3) Å] is significantly shortened compared to the neutral compound [1.541(4) Å]. This value is comparable to the C–C distance of the vicinal dication of diprotonated oxalic acid [1.528(3) Å].[9] The interatomic contacts of $[C_3H_4N_2O_3][AsF_6]_2$·4HF (**3**) are illustrated in Figure 2. The cation is connected with the anions, N1–(H1)···F4ii [2.765(2) Å], and HF molecules via moderate hydrogen bonds according to the classification by *Jeffrey*.[10] The hydrogen bonds via the HF molecules range between 2.449(2) Å and 2.511(1) Å, and are classified as strong to moderate.[10]
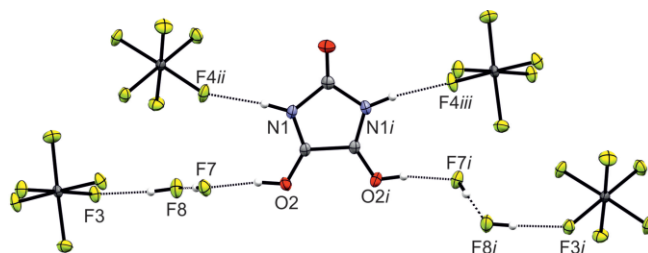
Figure 2. Projection of interatomic contacts in the $[C_3H_4N_2O_3][AsF_6]_2$·4HF (**3**) crystal (50 % probability displacement ellipsoids). Symmetry codes: $i = 1 - x$, y, $1.5 - z$; $ii = 0.5 + x$, $0.5 + y$, $1 + z$; $iii = 0.5 - x$, $- 0.5 + y$, $0.5 - z$. All contacts are drawn as dashed lines.

The As–F bond lengths of the AsF_6^- anions are in a range between 1.701(9) and 1.740(9) Å, which is in accordance with the literature.[11–13]

Crystal Structure of $[C_3H_3N_2O_3][SbF_6]$ (2)

The monoprotonated species of parabanic acid $[C_3H_3N_2O_3]$-$[SbF_6]$ (**2**) crystallizes in the monoclinic space group $P2_1/c$ with four formula units per unit cell. Figure 3 shows the asymmetric unit and Table 2 summarizes selected bond lengths and angles.
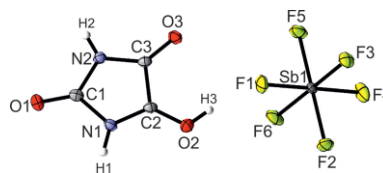
Figure 3. Asymmetric unit of $[C_3H_3N_2O_3][SbF_6]$ (**2**) (50 % probability displacement ellipsoids).

Even if the proton is not of great significance, it was found in the difference Fourier synthesis and refined isotropically. Compared to the neutral compound the C2–O2 bond length is significantly elongated [1.264(4) Å], which confirms the O-protonation.[7] Consequently, the N1–C2 distance [1.303(4) Å] is significantly shorter and in the range of the bond length of the diprotonated species. The other bond lengths of the two carbonyl groups are shortened to 1.183(4) Å for O1–C1 and 1.194(4) Å for C3–O3. A comparison of the most important bond lengths of parabanic acid, the monocation (**2**) and the dication (**3**) are summarized in Table 3.

EurJOC
European Journal of Organic Chemistry

Full Paper
doi.org/10.1002/ejoc.202000656

Chemistry Europe
European Chemical
Societies Publishing

Table 2. Selected bond lengths [Å] and angles [°] of (**2**). The estimated standard deviation is marked in parentheses.[a]

Bond lengths [Å]			
O1–C1	1.183(4)	N2–C3	1.361(4)
C1–N1	1.438(3)	C3–O3	1.194(4)
C1–N2	1.390(4)	C2–O2	1.264(4)
N1–C2	1.303(4)	C2–C3	1.524(4)
Bond angles [°]			
O1–C1–N1	125.6(3)	O2–C2–C3	126.2(3)
C1–N1–C2	110.6(2)	C2–C3–N2	103.4(2)
N1–C2–C3	108.1(2)	O3–C3–C2	124.9(3)
O2–C2–N1	125.6(3)	O3–C3–N2	131.6(3)
Interatomic contacts D–A [Å]			
O2–(H3)•••F1	2.555(3)	N1–(H1)•••F6i	2.927(3)
N2–(H2)•••F2ii	2.840(3)		

[a] Symmetry codes: $i = 1 - x, -y, 1 - z$; $ii = 1 + x, 0.5 - y, 0.5 + z$.

Table 3. Comparison of selected bond lengths [Å] of parabanic acid, (**2**) and (**3**) with estimated standard deviation in parentheses.[a]

	Parabanic acid[7]	(**2**)	(**3**)
O1–C1	1.212(4)	1.183(4)	1.167(3)
C1–N1	1.381(3)	1.438(3)	1.434(2)
N1–C2	1.360(3)	1.303(4)	1.305(2)
C2–O2	1.212(3)	1.264(4)	1.253(2)
C2–C(3/i)	1.541(4)	1.524(4)	1.511(3)

[a] Symmetry code: $i = 1 - x, y, 1.5 - z$.

The Sb–F bond lengths of the SbF_6^- anion are in a range between 1.866(2) and 1.895(2) Å. The angles are between 88.36(8) and 92.83(8)°, and between 176.47(8) and 179.77(8)°. These values are in good agreement with those reported in literature.[13,14] Deviations from perfect octahedron symmetry are explained by interatomic contacts, which are depicted in Figure 4.
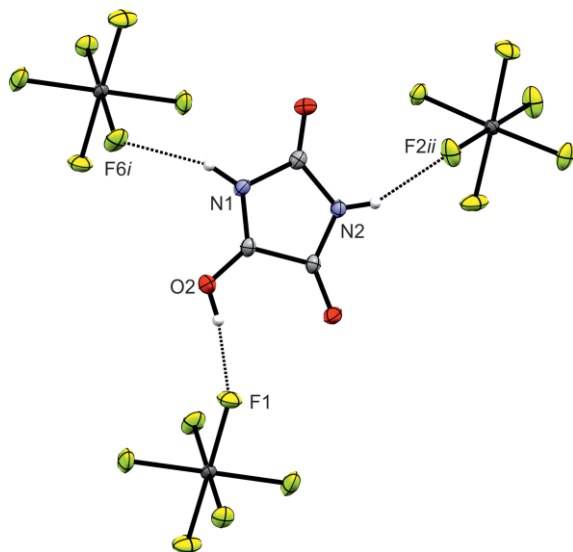
Figure 4. Projection of interatomic contacts in the $[C_3H_3N_2O_3][SbF_6]$ (**2**) crystal (50 % probability displacement ellipsoids). Symmetry codes: $i = 1 - x, -y, 1 - z$; $ii = 1 + x, 0.5 - y, 0.5 + z$.

The monocation is connected to the anions via moderate hydrogen bonds [O2–(H3)•••F1, N2–(H2)•••F2ii] with a distance of

2.555(3) Å, respectively 2.840(3) Å and via a weak hydrogen bond [N1–(H1)•••F6i] of 2.927(3) Å.

Vibrational Spectra of $[C_3X_4N_2O_3][MF_6]_2$ (M = As, Sb and X = H, D)

The infrared and Raman spectra of $[C_3H_4N_2O_3][AsF_6]_2$ (**3**), $[C_3H_4N_2O_3][SbF_6]_2$ (**4**) and $[C_3D_4N_2O_3][AsF_6]_2$ (**6**) as well as the Raman spectrum of parabanic acid are displayed in Figure 5.
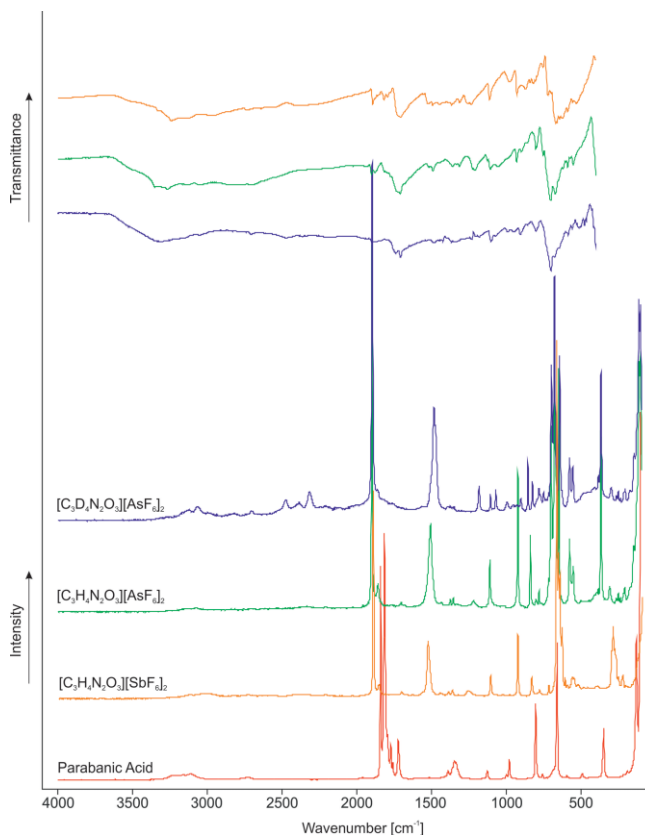
Figure 5. Raman spectrum of parabanic acid (red), Raman and IR spectra of $[C_3H_4N_2O_3][SbF_6]_2$ (**4**) (orange), $[C_3H_4N_2O_3][AsF_6]_2$ (**3**) (green) and $[C_3D_4N_2O_3][AsF_6]_2$ (**6**) (blue).

Table 4 lists selected observed frequencies of (**3**), (**4**) and (**6**) together with quantum-chemically calculated frequencies of $[C_3H_4N_2O_3]^{2+}\cdot 4HF$ and $[C_3D_4N_2O_3]^{2+}\cdot 4HF$. In Table S1 all observed and calculated frequencies are summarized (see Supporting Information). For better accordance of the calculated frequencies with observed ones, four HF molecules were added to the gas-phase structure, to simulate hydrogen bonding in the solid state.

According to the quantum chemical calculations, which are discussed later, the dication possesses C_{2v} symmetry with 30 fundamental vibrations. The successful diprotonation of parabanic acid is confirmed by the OH stretching vibrations in the infrared spectra [3128 cm^{-1}, 3043 cm^{-1} (**3**) and 3138 cm^{-1}, 2964 cm^1 (**4**)]. In the corresponding Raman spectra, these vibrations are not observable due to the poor polarizability. In contrast, the OD stretching vibrations are detected at 2322 cm^{-1}

EurJOC
European Journal of Organic Chemistry

Full Paper
doi.org/10.1002/ejoc.202000656

Chemistry
Europe
European Chemical
Societies Publishing

Table 4. Selected experimental vibrational frequencies [cm^{-1}] of (3), (4) and (6), and calculated vibrational frequencies [cm^{-1}] of $[C_3H_4N_2O_3]^{2+} \cdot 4HF$ and $[C_3D_4N_2O_3]^{2+} \cdot 4HF$.

| [C$_3$H$_4$N$_2$O$_3$][AsF$_6$]$_2$ (3) | | [C$_3$H$_4$N$_2$O$_3$][SbF$_6$]$_2$ (4) | | [C$_3$D$_4$N$_2$O$_3$][AsF$_6$]$_2$ (6) | | [C$_3$H$_4$N$_2$O$_3$]$^{2+}$·4HF Calc.[a] (IR/Raman) | [C$_3$D$_4$N$_2$O$_3$]$^{2+}$·4HF Calc.[a] (IR/Raman) | Assignment[b] |
IR	Raman	IR	Raman	IR	Raman			
3348 (w)		3327 (vw)		2476 (sh)	2474 (6)	3141 (305/272)	2333 (197/110)	ν(NX)
3267 (w)		3236 (w)		2382 (s)	2387 (5)	3103 (2937/44)	2293 (1533/21)	ν(NX)
3128 (w)		3138 (w)		2322 (s)	2318 (8)	2854 (1023/154)	2092 (563/69)	ν(OX)
3043 (w)		2964 (vw)				2823 (3999/88)	2071 (2017/39)	ν(OX)
1902 (vw)	1902 (100)	1894 (w)	1898 (58)	1898 (vw)	1899 (100)	1953 (132/114)	1948 (120/121)	ν(CO)
1772 (vw)		1774 (vw)				1768 (161/1)	1756 (180/2)	ν(CN)
1711 (m)	1707 (2)	1709 (m)	1709 (2)	1732 (w)		1764 (888/0.08)	1744 (906/0.4)	ν(CN)
1516 (vw)	1510 (19)	1518 (vw)	1533 (16)	1487 (vw)	1487 (32)	1507 (175/60)	1449 (29/71)	ν(CO)
	1379 (3)		1395 (2)	1182 (w)	1186 (10)	1417 (0.9/2)	1182 (66/5)	δ(CNX)
1452 (vw)		1448 (w)	1450 (2)		1377 (4)	1455 (0.7/1)	1385 (0.06/0.5)	ν(CO)
1360 (vw)	1359 (3)	1365 (w)	1371 (2)	995 (vw)	997 (5)	1280 (336/6)	968 (225/2)	δ(COX)
1225 (vw)	1224 (2)	1234 (w)	1265 (2)	959 (vw)	958 (5)	1269 (110/2)	956 (30/2)	δ(COX)
1107 (w)	1115 (11)	1113 (w)	1115 (7)	1107 (vw)	1110 (8)	1093 (218/9)	1016 (165/5)	ν(CN)
932 (w)	927 (30)	930 (w)	933 (18)	858 (w)	859 (w)	942 (70/13)	839 (34/10)	ν(CN)

[a] Calculated on the B3LYP/aug-cc-pVTZ level of theory. IR intensity in km/mol and Raman intensity in Å^4/u. Abbreviations for IR intensities: v = very, s = strong, m = medium, w = weak. Experimental Raman activities are stated to a scale of 1 to 100. [b] X = H, D.

(Ra) and 2318 cm^{-1} (IR) (6). Other than the mentioned ν(OD), also ν(ND) vibrations are observed [2476 cm^{-1}, 2382 cm^{-1} (IR) and 2474 cm^{-1}, 2387 cm^{-1} (Ra)], which is explained by H/D exchange at the NH groups. The H/D-red-shifts are in good agreement with the Teller-Redlich rule for an H/D isotopic effect.[15] Due to the twofold protonation on the neighboring carbonyl groups, the corresponding CO stretching vibrations are red shifted up to 342 cm^{-1} compared to the neutral compound.[16] They occur between 1448 cm^{-1} [IR, (4)] and 1533 cm^{-1} [Ra, (4)]. In contrast to the CO stretching vibrations, a blue shift of about 420 cm^{-1} is detected for the ν(CN) vibrations, compared to parabanic acid[16] {1707 cm^{-1} [Ra, (3)] and 1774 cm^{-1} [IR, (4)]}. The most intense line in the Raman spectra belongs to the remaining unprotonated carbonyl group, which occurs at approximately 1900 cm^{-1}. This value is remarkably high for a carbonyl group and is based on the strengthening of the bond, which is also observed in the crystal structure. For the anions AsF$_6^-$ and SbF$_6^-$, more than three lines are observed in the Raman spectra and likewise more than two bands in the infrared spectra. This is explained by a distortion of the ideal O_h symmetry, caused by solid state interactions.

The Raman and infrared spectra of the monoprotonated species [C$_3$H$_3$N$_2$O$_3$][AsF$_6$] (1), [C$_3$H$_3$N$_2$O$_3$][SbF$_6$] (2) and [C$_3$D$_3$N$_2$O$_3$][AsF$_6$] (5) are shown in Figure S1 and the observed and calculated frequencies are listed in Table S2 (see Supporting Information).

Theoretical Calculations

All theoretical calculations were carried out on the B3LYP/aug-cc-pVTZ level of theory with the Gaussian program package. Figure 6 shows the comparison of the calculated structure of [C$_3$H$_3$N$_2$O$_3$]$^+$ and the cation of the single-crystal X-ray structure of (2) together with bond lengths and angles. Comparing the values of the experimentally obtained geometric parameters of the [C$_3$H$_3$N$_2$O$_3$]$^+$ cation with the calculated ones, shows that almost all bond lengths and angles are in accordance. Only the N1–C1, as well as the C3–N2 bond lengths are calculated

slightly longer, compared to the experimental values. The C2–C3 distance is also predicted to be slightly longer by the calculation, than it is observed in the crystal structure.
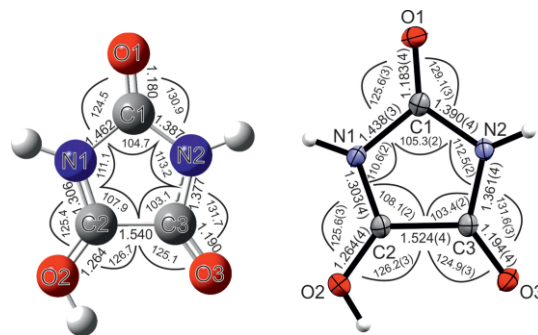
Figure 6. Calculated structure of [C$_3$H$_3$N$_2$O$_3$]$^+$ (left) and the [C$_3$H$_3$N$_2$O$_3$]$^+$ cation of the single-crystal X-ray structure (right) together with bond lengths [Å] and angles [°].

In Figure 7, the calculated structure of [C$_3$H$_4$N$_2$O$_3$]$^{2+}$ and the dication of the single-crystal X-ray structure are illustrated. In general, the calculated and experimentally obtained parameters of [C$_3$H$_4$N$_2$O$_3$]$^{2+}$ are in good agreement. As observed in the monocationic species, the same bond lengths (C1–N1 and
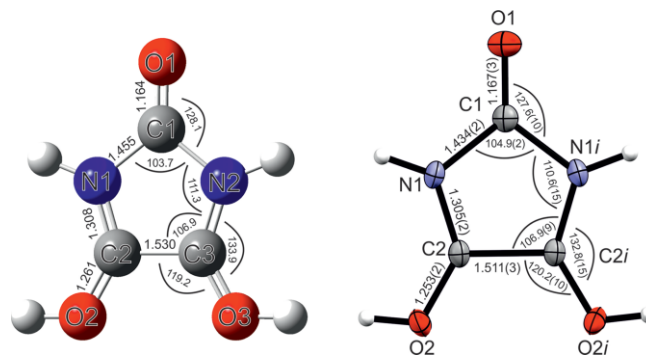
Figure 7. Calculated structure of [C$_3$H$_4$N$_2$O$_3$]$^{2+}$ (left) and the [C$_3$H$_4$N$_2$O$_3$]$^{2+}$ cation of the single-crystal X-ray structure (right) together with bond lengths [Å] and angles [°].

EurJOC
European Journal of Organic Chemistry

Full Paper
doi.org/10.1002/ejoc.202000656

Chemistry Europe
European Chemical Societies Publishing

C2–C3) are slightly elongated in the calculated structure of $[C_3H_4N_2O_3]^{2+}$ compared to the single-crystal X-ray structure.

Mapped Electrostatic Potentials (MEPs) together with Natural Population Analysis charges (NPA) are calculated to analyze where the positive charges of the diprotonated species are located. Figures 8, 9 and 10 depict the MEPs together with the NPA of parabanic acid, $[C_3H_4N_2O_3]^{2+}$ and $[C_3H_4N_2O_3]^{2+} \cdot 4HF$. The calculation for parabanic acid shows that the positive electrostatic potential is located inside the entire five-membered ring structure. The negative electrostatic potential is located exclusively on the oxygen atoms (red), which highlights the carbonyl groups as the more attractive functional group for protonation compared to the amide groups. Positive NPA charges are found at all carbon atoms, whereas the negative ones are observed for all oxygen and nitrogen atoms. Twofold protonation of parabanic acid leads to a change of the electrostatic potential distribution. The positive potential (blue) is now located between the two neighboring carbon atoms. In contrast, the negative potential is strongly compacted at the unprotonated oxygen atom. The influence on the NPA charges is describable as an increase of the positive carbon atom charges and a decrease of the negative oxygen and nitrogen atom charges. This leads to the assumption that both positive charges are delocalized over the individual OCNCO site of the molecule. The addition of four HF molecules for the simulation of hydrogen bonds in the solid-state results in a similar delocalization of the positive charges. Interestingly, a different trend is observed for the NPA charges of O2 and O3 atoms, which are decreased compared to the values of parabanic acid. Consequently, the NPA charges for the carbon atoms increase, whilst they decrease for the nitrogen atoms, however slightly weaker. By adding four HF molecules, the positive electrostatic potential is more distributed over the ring structure, but nevertheless compacted at C2 and C3. In conclusion, these calculations show that the two positive charges are located on the two carbon atoms C2 and C3, even though the charges are slightly compensated by the neighboring oxygen and nitrogen atoms. Albeit a 1,3-*N,N* dication would appear more stable due to the larger distance of the positive charges, a 1,2-*C,C* dication is generated by the twofold protonation of parabanic acid. The synthesized dicarbenium dication represents a new compound, which is to classify into 1,2 dications in organic main group systems.[17]
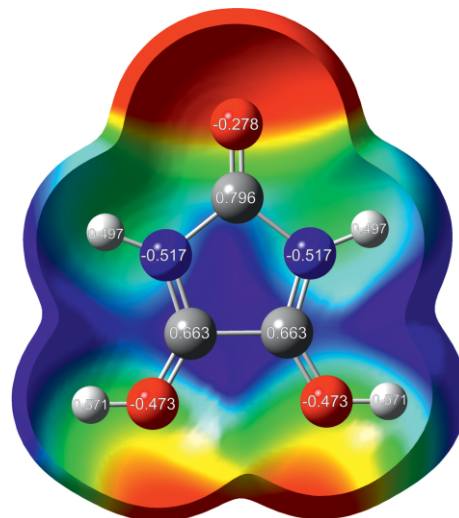
Figure 9. Molecular 0.0004 bohr^{-3} 3D isosurfaces with mapped electrostatic potential as a color scale ranging from 0.28 a.u. (red) to 0.37 a.u. (blue). The electrostatic potential isosurfaces and the NPA charges have been calculated for $[C_3H_4N_2O_3]^{2+}$.
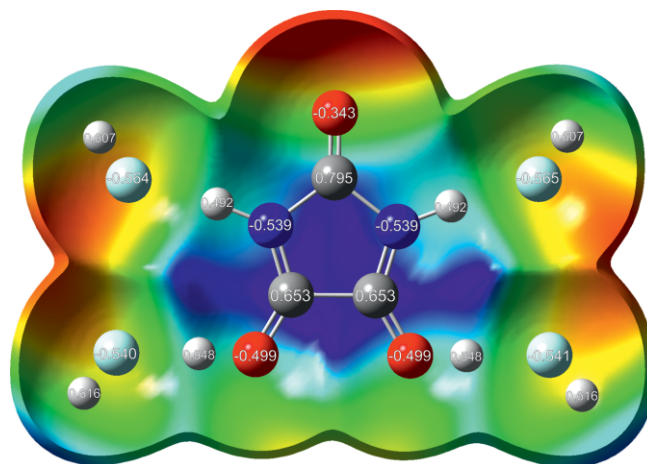
Figure 10. Molecular 0.0004 bohr^{-3} 3D isosurfaces with mapped electrostatic potential as a color scale ranging from 0.20 a.u. (red) to 0.31 (blue). The electrostatic potential isosurfaces and the NPA charges have been calculated for $[C_3H_4N_2O_3]^{2+} \cdot 4HF$.

Figure 8. Molecular 0.0004 bohr^{-3} 3D isosurfaces with mapped electrostatic potential as a color scale ranging from –0.03142 a.u. (red) to 0.05124 a.u. (blue). The electrostatic potential isosurfaces and the NPA charges have been calculated for $C_3N_2O_3H_2$.

Conclusion

Parabanic acid was investigated in the superacidic systems XF/MF$_5$ (X = H, D; M = As, Sb) for the first time. Using an equimolar amount of Lewis acid with respect to the starting material, the formation of the monoprotonated species in terms of $[C_3H_3N_2O_3][AsF_6]$ (**1**), $[C_3H_3N_2O_3][SbF_6]$ (**2**) and the correspond-

EurJOC
European Journal of Organic Chemistry

Full Paper
doi.org/10.1002/ejoc.202000656

Chemistry Europe
European Chemical
Societies Publishing

ing deuterated compound $[C_3D_3N_2O_3][AsF_6]$ (**5**) is observed. A twofold or larger amount of Lewis acid generates the compounds $[C_3H_4N_2O_3][AsF_6]_2$ (**3**), $[C_3H_4N_2O_3][SbF_6]_2$ (**4**) and $[C_3D_4N_2O_3][AsF_6]_2$ (**6**). The compounds were isolated and characterized by IR and Raman spectroscopy. The spectroscopical results are supported by calculated vibrational frequencies on the B3LYP/aug-cc-pVTZ level of theory. In case of $[C_3H_3N_2O_3][SbF_6]$ (**2**) and $[C_3H_4N_2O_3][AsF_6]_2\cdot4HF$ (**3**) single-crystal X-ray structure analyses were performed. In the dicationic species both protonations were determined on the neighboring carbonyl groups. For determining where the two positive charges are located, Mapped Electrostatic Potentials and Natural Popular Analysis charges were calculated. The positive charges of the 1,2-*C,C* dication are slightly compensated by the neighboring nitrogen and oxygen atoms.

Experimental Section

General

Caution! Avoid contact with any of these compound. Hydrolysis might form HF, which burns skin and causes irreparable damage.

Apparatus and Materials

Standard Schlenk technique with a stainless steel vacuum line was used to perform all reactions. All reactions in superacidic media were carried out in FEP/PFA reactors closed with a stainless steel valve. The reactors as well as the vacuum line were dried with fluorine prior to use. A Bruker Vertex-80V FT-IR spectrometer ($\tilde{v}$ = 350 to 4000 cm^{-1}) was used for recording low-temperature IR spectra. Small amounts of the synthesized compounds were placed on a CsBr single-crystal plate in a cooled cell for the measurement. For Raman measurements, the samples were transferred into cooled glass cells (–196 °C), which were evacuated afterwards. The measurements were performed by a Bruker MultiRAM FT-Raman spectrometer with Nd:YAG laser excitation (λ = 1064 nm). The low-temperature X-ray diffraction of $[C_3H_3N_2O_3][SbF_6]$ (**2**) and $[C_3H_4N_2O_3][AsF_6]_2\cdot4HF$ (**3**) was performed with an Oxford X-Calibur3 equipped with a Kappa CCD detector, operating with Mo-K_α radiation (λ = 0.71073 Å) and a Spellman generator (voltage 50 kV, current 40 mA). The CrysAlis CCD software was used to collect the data at 130 K,[18] while the reduction was carried out using CrysAlis RED software.[19] Solution and refinement of the crystal structures were performed with programs SHELXS[20] and SHELXL-97,[21] belonging to the WinGX software package. Subsequently, the structure was verified by PLATON software.[22] SCALE ABSPACK multiscan method was used for absorption correction.[23] In Table S3 and S4 (see Supporting Information) selected data and parameters of the X-ray analysis are listed. The quantum chemical calculations were carried out on the B3LYP/aug-cc-pVTZ level of theory by Gaussian 09.[24]

Deposition Numbers 1995038 for $[C_3H_3N_2O_3]^+[SbF_6]^-$ (**2**) and 1995041 for $[C_3H_4N_2O_3][AsF_6]_2\cdot4HF$ (**4**) contain the supplementary crystallographic data for this paper. These data are provided free of charge by the joint Cambridge Crystallographic Data Centre and Fachinformationszentrum Karlsruhe Access Structures service www.ccdc.cam.ac.uk/structures.

Synthesis of $[C_3H_3N_2O_3][AsF_6]$ (1), $[C_3H_4N_2O_3][AsF_6]_2$ (3) $[C_3D_3N_2O_3][AsF_6]$ (5) and $[C_3D_4N_2O_3][AsF_6]_2$ (6): Anhydrous hydrogen fluoride (2 mL) was condensed into an FEP tube-reactor at –196 °C. For compounds (**5**) and (**6**) deuterium fluoride was used instead. Afterwards, arsenic pentafluoride [85 mg, 0.5 mmol for (**1**)

and (**5**), and 170 mg, 1.0 mmol for (**3**) and (**6**)] was condensed in the tube-reactor under same conditions. To form the superacidic systems, the mixtures were warmed up to –40 °C and homogenized, subsequently. After cooling down again to –196 °C, parabanic acid (57 mg, 0.5 mmol) was added under nitrogen atmosphere. After warming up to –40 °C [(**1**), (**5**)], or –60 °C [(**3**), (**6**)] respectively, the reaction mixture was homogenized until the resulted salt was completely dissolved. The solution was again cooled to –196 °C and excess HF or DF was removed under dynamic vacuum overnight at –78 °C. For crystallization of compound (**3**), the reactor was left in an ethanol bath (*T* = –70 °C) without removing HF until the salt recrystallized. All salts were obtained as colorless solids. $[C_3H_3N_2O_3][AsF_6]$ (**1**), and $[C_3D_3N_2O_3][AsF_6]$ (**5**) are stable up to room temperature, whereas $[C_3H_4N_2O_3][AsF_6]_2$ (**3**) and $[C_3D_4N_2O_3]$-$[AsF_6]_2$ (**6**) were decomposed at –20 °C.

Synthesis of $[C_3H_3N_2O_3][SbF_6]$ (2) and $[C_3H_4N_2O_3][SbF_6]_2$ (4): Antimony pentafluoride [110 mg, 0.51 mmol (**2**); 213 mg, 0.98 mmol (**4**)] was condensed into an FEP tube-reactor at –196 °C. Subsequently, 2 mL of anhydrous hydrogen fluoride were condensed into the reactor at –196 °C. For homogenizing these compounds, the reaction mixtures were warmed up to –40 °C. Under nitrogen atmosphere, parabanic acid [58 mg, 0.51 mmol (**2**), 56 mg, 0.49 mmol (**4**)], was added to the refrozen superacidic system. The complete reaction mixture was warmed up to –40 °C (**2**), –60 °C respectively (**4**), and was homogenized until the salt was completely dissolved. Excess HF was removed under dynamic vacuum at –78 °C, after the solution had been cooled down to –196 °C. Both compounds were obtained as colorless solids with decomposition temperatures of 20 °C for $[C_3H_3N_2O_3][SbF_6]$ (**2**) and –20 °C for $[C_3H_4N_2O_3][SbF_6]_2$ (**4**). For crystallization of compound (**2**), the reactor was left in an ethanol bath (*T* = –50 °C) until the salt recrystallized.

[1] F. Woehler, J. Liebig, *Ann. Pharm.* **1838**, *26*, 256.
[2] P. H. Laursen, W. A. Thews, B. E. Christensen, *J. Org. Chem.* **1957**, *22*, 274.
[3] J. I. Murray, *Org. Synth.* **1957**, *37*, 71.
[4] E. S. Canellakis, A. L. Tuttle, P. P. Cohen, *J. Biol. Chem.* **1955**, *213*, 397.
[5] M. d. D. M. C. Ribeiro da Silva, M. A. V. Ribeiro da Silva, V. L. S. Freitas, M. V. Roux, P. Jiménez, J. Z. Dávalos, P. Cabildo, R. M. Claramunt, J. Elguero, *J. Chem. Thermodyn.* **2008**, *40*, 1378.
[6] M. Arca, F. Demartin, F. A. Devillanova, F. Isaia, F. Lelj, V. Lippolis, G. Verani, *Can. J. Chem.* **2000**, *78*, 1147.
[7] D. R. Davies, J. J. Blum, *Acta Crystallogr.* **1955**, *8*, 129.
[8] A. F. Holleman, E. Wiberg, N. Wiberg, *Anorganische Chemie*, De Gruyter, Berlin, Boston, **2017**.
[9] M. Schickinger, T. Saal, F. Zischka, J. Axhausen, K. Stierstorfer, Y. Morgenstern, A. J. Kornath, *ChemistrySelect* **2018**, *3*, 12396.
[10] G. A. Jeffrey, *An Introduction to hydrogen bonding*, Oxford University Press, New York, **1997**.
[11] R. Minkwitz, F. Neikes, U. Lohmann, *Eur. J. Inorg. Chem.* **2002**, *2002*, 27.
[12] K. O. Christe, X. Zhang, R. Bau, J. Hegge, G. A. Olah, G. K. S. Prakash, J. A. Sheehy, *J. Am. Chem. Soc.* **2000**, *122*, 481.

[13] M. Schickinger, C. Jessen, Y. Morgenstern, K. Muggli, F. Zischka, A. Kornath, *Eur. J. Org. Chem.* **2018**, *2018*, 6223.

[14] R. Minkwitz, S. Schneider, *Angew. Chem. Int. Ed.* **1999**, *38*, 210; *Angew. Chem.* **1999**, *111*, 229.

[15] J. Weidlein, K. Dehnicke, U. Müller, *Schwingungsspektroskopie. Eine Einführung*, Thieme, Stuttgart, **1988**.

[16] L. Coclers, A. Vanclef, R. Bouché, *Spectrosc. Lett.* **1978**, *11*, 799.

[17] V. G. Nenajdenko, N. E. Shevchenko, E. S. Balenkova, I. V. Alabugin, *Chem. Rev.* **2003**, *103*, 229.

[18] *CrysAlisCCD*, Version 1.171.35.11 (release 16–05–**2011** CrysAlis 171.NET), Oxford Diffraction Ltd., **2011**.

[19] *CrysAlisRED*, Version 1.171.35.11 (release 16.05.**2011** CrysAlis 171.NET), Oxford Diffraction Ltd., **2011**.

[20] G. Sheldrick, *SHELXS-97, Program for Crystal Structure Solution*, University of Göttingen, Germany, **1997**.

[21] G. Sheldrick, *SHELXL-97, Program for the Refinement of Crystal Structures*, University of Göttingen, Germany, **1997**.

[22] A. Spek, *PLATON, A Multipurpose Crystallographic Tool*, Utrecht University, Utrecht (The Netherlends), **1999**.

[23] *SCALE3 ABSPACK* - An Oxford Diffraction Program, Oxford Diffraction Ltd., UK, **2005**.

[24] M. J. Frisch, G. W. Trucks, H. B. Schlegel, G. E. Scuseria, M. A. Robb, J. R. Cheeseman, G. Scalmani, V. Barone, B. Mennucci, G. A. Petersson, H. Nakatsuji, M. Caricato, X. Li, H. P. Hratchian, A. F. Izmaylov, J. Bloino, G. Zheng, J. L. Sonnenberg, M. Hada, M. Ehara, K. Toyota, R. Fukuda, J. Hasegawa, M. Ishida, T. Nakajima, Y. Honda, O. Kitao, H. Nakai, T. Vreven, J. A. Montgomery Jr., J. E. Peralta, F. Ogliaro, M. Bearpark, J. J. Heyd, E. Brothers, K. N. Kudin, V. N. Staroverov, R. Kobayashi, J. Normand, K. Raghavachari, A. Rendell, J. C. Burant, S. S. Iyengar, J. Tomasi, M. Cossi, N. Rega, J. M. Millam, M. Klene, J. E. Knox, J. B. Cross, V. Bakken, C. Adamo, J. Jaramillo, R. Gomperts, R. E. Stratmann, O. Yazyev, A. J. Austin, R. Cammi, C. Pomelli, J. W. Ochterski, R. L. Martin, K. Morokuma, V. G. Zakrzewski, G. A. Voth, P. Salvador, J. J. Dannenberg, S. Dapprich, A. D. Daniels, Ö. Farkas, J. B. Foresman, J. V. Ortiz, J. Cioslowski, D. J. Fox, *Gaussian 09, Revision A.02*, Gaussian, Inc., Wallingford CT, **2009**.